



OPEN ACCESS

EDITED BY

Olga Solomina,
Institute of Geography (RAS), Russia

REVIEWED BY

Feng Chen,
Yunnan University, China
Keyan Fang,
Fujian Normal University, China

*CORRESPONDENCE

Dominik Florian Stangler
dominik.stangler@wwd.uni-freiburg.de

SPECIALTY SECTION

This article was submitted to
Paleoecology,
a section of the journal
Frontiers in Ecology and Evolution

RECEIVED 29 March 2022

ACCEPTED 15 August 2022

PUBLISHED 23 September 2022

CITATION

Stangler DF, Miller TW, Honer H,
Larysch E, Puhlmann H, Seifert T and
Kahle H-P (2022) Multivariate drought
stress response of Norway spruce,
silver fir and Douglas fir along
elevational gradients in Southwestern
Germany.
Front. Ecol. Evol. 10:907492.
doi: 10.3389/fevo.2022.907492

COPYRIGHT

© 2022 Stangler, Miller, Honer,
Larysch, Puhlmann, Seifert and Kahle.
This is an open-access article
distributed under the terms of the
[Creative Commons Attribution License
\(CC BY\)](https://creativecommons.org/licenses/by/4.0/). The use, distribution or
reproduction in other forums is
permitted, provided the original
author(s) and the copyright owner(s)
are credited and that the original
publication in this journal is cited, in
accordance with accepted academic
practice. No use, distribution or
reproduction is permitted which does
not comply with these terms.

Multivariate drought stress response of Norway spruce, silver fir and Douglas fir along elevational gradients in Southwestern Germany

Dominik Florian Stangler^{1*}, Tobias Walter Miller¹,
Harald Honer¹, Elena Larysch¹, Heike Puhlmann²,
Thomas Seifert^{1,3} and Hans-Peter Kahle¹

¹Chair of Forest Growth and Dendroecology, Institute of Forest Sciences, University of Freiburg, Freiburg, Germany, ²Department of Soil and Environment, Forest Research Institute Baden-Württemberg, Freiburg, Germany, ³Department for Forest and Wood Science, Stellenbosch University, Matieland, South Africa

The conifer tree species Norway spruce (*Picea abies*), silver fir (*Abies alba*) and Douglas fir (*Pseudotsuga menziesii*) are important elements in tree species composition and forest management of Central European forests, but their potential to thrive under anticipated climatic changes is still debated controversially. This study contributes a multivariate analysis of resilience components based on increment cores sampled at breast height of Norway spruce, silver fir and Douglas fir trees growing along elevational gradients in Southwestern Germany. We aimed to gain novel insights into the species-specific and elevational response of tree growth and wood density variables during the extreme drought events of the years 2003 and 2018. Our results for Norway spruce corroborate projections of its ongoing decline during climate change as the reductions of wood density and biomass production indicated high drought sensitivity at all elevations. Moreover, resilience indices of mean tree-ring density, maximum latewood density, tree-ring width and biomass production were even lower after the drought of 2018 compared to the previous drought of 2003. Silver fir, a potential substitute tree species for Norway spruce, showed unexpected results with resistance and resilience indices being significantly lower in 2018 compared to 2003 indicating that silver fir might be more vulnerable to drought than previously expected, especially at low elevations. In contrast, the superior growth rates and higher levels of drought tolerance of Douglas fir were especially pronounced during the drought of 2018 and visible across the entire elevational gradient, even though high coning intensity was present for all investigated tree species as a possible confounding factor to exacerbate the drought stress effects in the study region.

KEYWORDS

carbon sequestration, wood density, drought, conifers, resistance, resilience

Introduction

Norway spruce (*Picea abies* (L.) Karst.), silver fir (*Abies alba* Mill.) and Douglas fir (*Pseudotsuga menziesii* (Mirb.) Franco) form important elements in tree species composition and forest management of Central European forests (San-Miguel-Ayanz et al., 2016; Spiecker et al., 2019). Due to their high productivity and favorable wood technological properties for timber construction (Kohnle et al., 2011; Henin et al., 2019), their lumber offers high substitution potential to replace energy-intensive materials such as steel or concrete and serves as medium to long-term carbon storage (Leskinen et al., 2018).

According to the most recent National Forest Inventory, Norway spruce is the most widespread tree species in Germany and covers 25% of the national forest area (BMEL, 2014). Despite its paramount importance for the current forest and wood sector, growth and vitality of Norway spruce is projected to decline with further climate change (Vitali et al., 2018; Brandl et al., 2020), due to its high drought sensitivity and susceptibility to biotic and abiotic stressors (Bolte et al., 2009; van der Maaten-Theunissen et al., 2013; Vitali et al., 2017). These risks are especially high, when spruce is planted on sites located outside the dry-warm borders of its climate envelope (Kahle, 2006; Hartl-Meier et al., 2014). Silver fir is a native tree species of the potential natural vegetation of predominantly mountainous forest ecosystems in Central Europe (Vitasse et al., 2019). It has been frequently proposed as a potential substitute tree species for Norway spruce as it is presumably more drought tolerant, better adapted to the changing climatic conditions and might even benefit from global warming at high elevation sites (van der Maaten-Theunissen et al., 2013; Hartl-Meier et al., 2014; Vitali et al., 2018; Vitasse et al., 2019). In contrast, more recent studies demonstrated surprisingly low growth resistance as well as unexpected vulnerability and mortality of silver fir in response to the extreme drought anomaly in 2018 (Schuldt et al., 2020; Larysch et al., 2021). Douglas fir is a highly productive tree species originating from the Pacific Northwest of North America and has been successfully introduced and managed in Central European forests since the 19th century (Kohnle et al., 2019; van Loo and Dobrowolska, 2019). Previous studies provided evidence of the superior capacity of Douglas fir to cope with extreme drought conditions and its simultaneous potential to maintain higher growth rates than co-occurring conifers (Eilmann and Rigling, 2012; Vitali et al., 2017). However, survival probability of Douglas fir in the context of anticipated climatic changes is critically discussed and its suitability to replace Norway spruce on low elevation sites is debated (Vejpustková and Čihák, 2019; Brandl et al., 2020; Maringer et al., 2021).

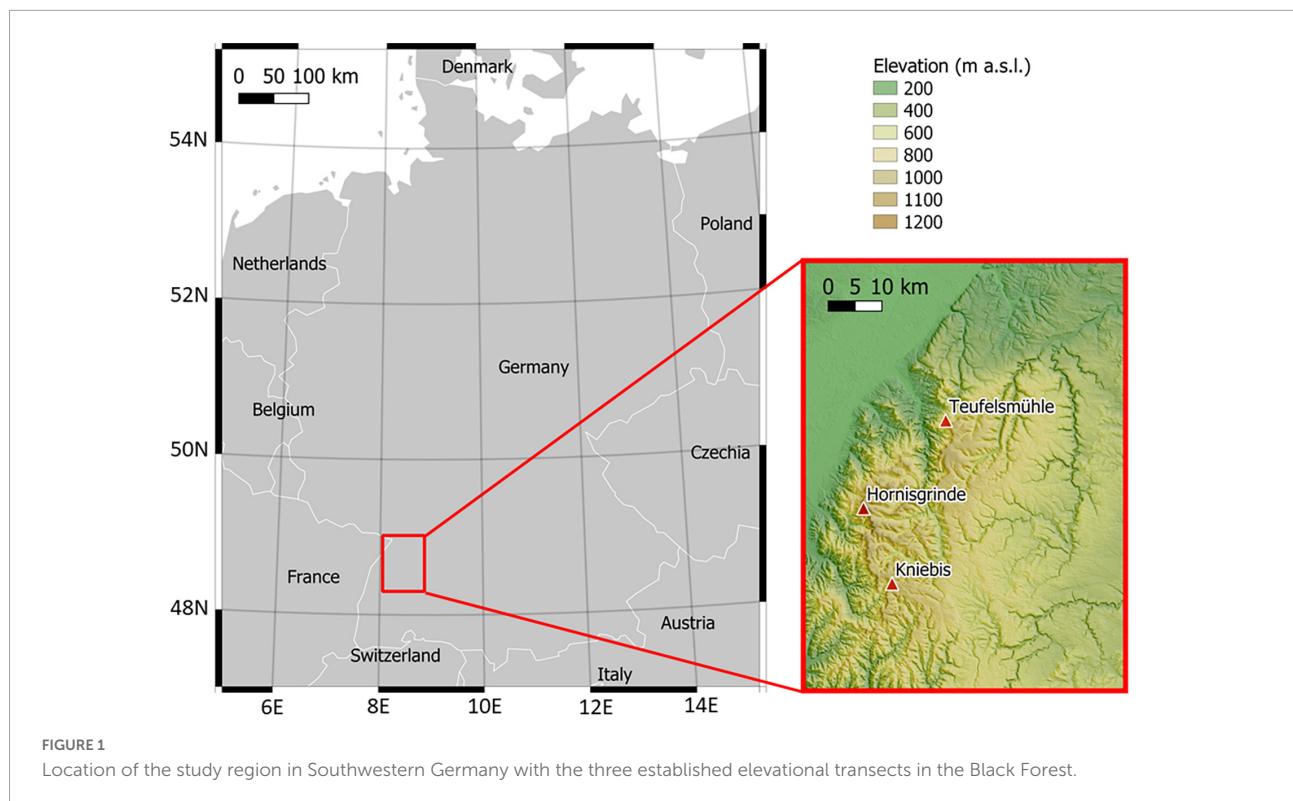
For the assessment of short-term responses of tree growth to extreme climatic events such as the summer drought anomalies in 2003 or 2018, the analysis of drought tolerance indices as introduced by Lloret et al. (2011) became increasingly popular

during the last decade (Montwé et al., 2015; Vitali et al., 2017; Schmied et al., 2022). The concept is usually based on the relationships of tree-ring growth before, during and after the extreme event. Based on these relationships, indices of resistance, recovery and resilience are calculated to evaluate and compare drought stress tolerance of tree species (Diaconu et al., 2017). Additional growth variables such as maximum latewood density are frequently integrated in dendroecological analyses due their well-known sensitivity to growing season temperatures (Conkey, 1979; Büntgen et al., 2007; van der Maaten-Theunissen et al., 2012). However, their integration into the analyses of drought tolerance indices still bears great potential to provide novel insights into short-term tree growth responses to extreme climatic events (Schwarz et al., 2020). Wood density is a key parameter with paramount importance for carbon sequestration and woody biomass production as well as for wood quality including various wood technological properties such as hardness and mechanical stability or calorific value (Wassenberg et al., 2015a). In addition, wood density has been frequently associated with the resistance of the xylem hydraulic architecture against embolism and hydraulic failure during drought (Martinez-Meier et al., 2008; Rosner et al., 2014; Luss et al., 2019).

This study contributes a dendroecological analysis based on increment cores sampled at breast height of Norway spruce, silver fir and Douglas fir trees in the Black Forest in Southwestern Germany. By means of semi-automatic image analysis and measurements of intra-annual density profiles, we developed time series of tree-ring width, mean tree-ring density and maximum latewood density as well as stem radial biomass increment from 108 sample trees growing along three elevational gradients. Using this data, we performed a multivariate analysis of drought tolerance indices to gain novel insights into the species-specific and elevational response of tree growth and wood density variables to the recent extreme drought event of the year 2018 and aimed to validate previous conclusions on drought tolerance and suitability of silver fir and Douglas fir to replace Norway spruce on potentially drought-prone sites in Central Europe. The year 2018 was chosen for investigating drought stress tolerance as it was classified as one of the most severe drought events ever recorded in Central Europe (Schuldt et al., 2020), similar to the millennial drought year 2003, which we also included as baseline reference into the analysis (van der Maaten-Theunissen and Bouriaud, 2012; Vitali et al., 2017).

We hypothesized that:

- I. Norway spruce shows lower drought tolerance than silver fir and Douglas fir, in particular at low elevations.
- II. Species-specific differences in drought responses are similar for both drought events, 2003 and 2018.
- III. Before, during and after drought events, Douglas fir shows superior growth rates and higher wood density compared to silver fir and Norway spruce.



Materials and methods

Selection of study sites and sample trees

Study sites and sample trees were selected in winter 2018/2019 along three elevational transects within the northern part of the Black Forest, a mountain range located in Southwestern Germany (**Figure 1**). The three replications were established along the mountains Teufelsmühle (48° 45' 14" N, 8° 24' 30" E), Hornisgrinde (48° 36' 25" N, 8° 12' 9" E) and Kniebis (48° 28' 53" N, 8° 16' 33" E) with each tree species sampled at four research plots arranged at largely equidistant elevational levels. Research plots were selected in managed forest stands with low inter-specific competition located predominantly on northwest-facing slopes. Soil types at the research plots are predominantly cambisols with medium skeleton content and loamy soil textures. In each of the 36 investigated plots, three mature and vital sample trees without visible damages were selected from the dominant and co-dominant crown class with a total sample size of 108 trees (3 transects \times 3 species \times 4 plots \times 3 trees). The elevational transects represent ecological gradients from relatively dry and warm low elevation sites to cool and moist high elevation sites. Detailed information on the climatic conditions and the average stand- and tree-level characteristics for each species and elevational level are presented in **Table 1**.

Sampling and preparation of increment cores

One increment core of 5 mm diameter was extracted at breast height (1.3 m) from each sample trees using Haglöf borers (Haglöf Sweden AB, Långsele, Sweden) after the growing season 2020. Increment cores were sampled perpendicular to the direction of the slope to avoid compression wood. After drying, the increment cores were fixed in LC45 cable conduits (Hermann Kleinhuis GmbH + Co. KG, Linz am Rhein, Germany), mounted on glass plates and their cross-sections were prepared with an ultra-precise diamond fly cutter (Kugler F500, Kugler GmbH, Salem, Germany) producing highly smooth surfaces for subsequent wood density measurement with high-frequency (HF) densitometry (Spiecker et al., 2000; Schinker et al., 2003; Wassenberg et al., 2015b).

Measurements of tree-ring width and wood density

Image sequences with a resolution of 35.57 pixel mm^{-1} were taken of the prepared surfaces of the increment cores using a black and white camera mounted above a high-precision motorized linear positioning table moving in the radial direction from pith to bark (Wassenberg et al., 2015b). Tree-ring widths were measured on the stitched images perpendicular

TABLE 1 Sample size and mean values (with standard deviations in parentheses) of elevations, stand basal area, diameter at breast height (DBH), tree height, tree age at breast height ($t_{1.3}$) and slope for all sample trees grouped by species and elevational level.

Species	Elevational level	Elevation [m a.s.l.]	Stand basal area [m ² /ha]	No. of trees	DBH [cm]	Tree height [m]	$t_{1.3}$ [yrs]	Slope [°]	T air [°C]	P [mm]
Norway spruce	low	394 (17)	30.9 (5.4)	9	53.1 (3.4)	35.0 (2.3)	71.0 (2.9)	22 (9)	9.2 (0.9)	1543 (34)
	low-med	557 (21)	36.2 (5.1)	9	47.7 (3.5)	32.6 (2.9)	58.0 (4.9)	24 (6)	7.9 (0.5)	1720 (189)
	high-med	673 (27)	33.4 (4.9)	9	53.3 (11.7)	33.3 (4.2)	74.9 (24.7)	17 (6)	7.4 (0.9)	1803 (137)
	high	825 (11)	34.8 (5.1)	9	52.3 (5.6)	32.2 (2.1)	84.0 (19.8)	6 (6)	6.5 (0.3)	1819 (159)
Silver fir	low	413 (57)	28.9 (3.5)	9	54.3 (5.3)	32.4 (3.0)	82.1 (7.0)	6 (4)	9.3 (0.3)	1476 (122)
	low-med	560 (29)	35.6 (10.6)	9	55.4 (7.2)	30.8 (2.1)	73.1 (10.1)	23 (3)	8.6 (0.3)	1619 (148)
	high-med	686 (13)	35.5 (5.2)	9	56.3 (10.3)	31.0 (2.9)	83.4 (26.4)	23 (4)	7.3 (0.4)	1939 (54)
Douglas fir	low	359 (39)	26.5 (5.0)	9	68.4 (7.9)	42.1 (3.6)	69.2 (11.5)	24 (9)	9.2 (0.5)	1472 (30)
	low-med	523 (5)	32.8 (4.4)	9	64.3 (3.8)	39.4 (1.8)	60.9 (3.3)	18 (6)	8.6 (0.4)	1571 (58)
	high-med	674 (10)	30.2 (9.4)	9	64.0 (6.9)	35.3 (2.5)	57.6 (5.2)	14 (13)	7.9 (0.5)	1789 (102)
	high	807 (20)	33.6 (6.0)	9	74.9 (8.4)	40.0 (4.5)	88.0 (10.1)	8 (5)	6.7 (0.3)	1849 (136)

Mean annual temperature (T air) and annual precipitation sums (P) were modeled on the stand level using a 250 m grid according to [Dietrich et al. \(2019\)](#) and represent mean values of the climate normal period 1981–2010 for all selected stands within each of the elevational levels, respectively.

to the orientation of the ring boundaries using an in-house semi-automatic image analysis system of the Chair of Forest Growth and Dendroecology. Cross-dating of the measured tree-ring chronologies was conducted using the software package PAST4 ([Knibbe, 2004](#)). Intra-annual wood density profiles were measured in high resolution using HF densitometry, which measures the relative density variations (in mV) based on the propagation of an electromagnetic stray field emitted by an HF probe with a radial integration width of 175 μm ([Schinker et al., 2003](#); [Wassenberg et al., 2015b](#)). The HF probe moved over the wood surface on the exact same track as the acquired image sequences and recorded wood density variations from pith to bark every 26 μm . Data points measured in close proximity to adjacent tree-ring boundaries that contained signals of earlywood as well as latewood cells were removed from the individual intra-annual profiles according to the radial integration width of the HF probe ([Wassenberg et al., 2015b](#)). For tree-ring widths smaller than twice the radial integration width of 175 μm , we removed all points before the first local minimum and after the last maximum of the intra-annual profiles instead ([Sprengel et al., 2020](#)). HF densitometry measurements were finally converted from voltage to air-dry volumetric density in g cm^{-3} using daily updated linear calibration functions (average $R^2 > 0.93$) developed according to guidelines presented by [Wassenberg et al. \(2014\)](#).

Environmental data

For characterization of the average climatic conditions of the selected research plots during the climate normal period 1981–2010, data of the meteorological variables precipitation and air temperature were available in a 250 \times 250 m grid ([Dietrich et al., 2019](#)). As the higher resolution data of [Dietrich et al. \(2019\)](#) did not contain the post-drought years 2019 and 2020, we used environmental data in monthly resolution provided in a 1 \times 1 km grid by the German Meteorological Service ([DWD, 2022](#)) to classify the climatic conditions and

highlight periods of environmental stress during the pre-drought, drought and post-drought years of 2003 and 2018. To detect potential anomalies, the monthly mean values of air temperature, precipitation sums, climatic water balance and relative plant available water were calculated as deviations from their corresponding 30-year mean values and illustrated together with the 2.5 and 97.5% percentiles based on the baseline climate period 1991–2020 ([Figure 2](#)). The corresponding absolute values of the same environmental variables for the 30-year mean and the two drought events are presented in [Supplementary Figure 1](#).

Analysis of drought tolerance indices

All calculations and statistical data analyses were conducted in the R-programming environment ([R Core Team, 2022](#)). Besides the annual values of tree-ring width and maximum latewood density, we also calculated for each tree-ring the mean tree-ring density (\bar{d}) and estimated the annual stem radial biomass increment for the sampled increment cores using Equation 1:

$$rbi_{i,t} = \frac{\pi}{4} \times DC^2 \times RW_{i,t} \times \bar{d}_{i,t} \times CC \quad (1)$$

where rbi is the annual stem radial biomass increment in gC (grams carbon) of tree i in year t , DC represents the 0.5 cm diameter of the sampled increment core, RW denotes tree-ring width (in cm) and \bar{d} represents the corresponding mean air-dry tree-ring density (in g cm^{-3}), respectively, whereas CC represents carbon concentration, specified to be 50 % ([Lamloom and Savidge, 2003](#); [Thomas and Martin, 2012](#)).

We performed an analysis of drought tolerance indices as introduced by [Lloret et al. \(2011\)](#) to quantify and compare multivariate growth responses of the investigated tree species between the extreme drought years 2003 and 2018. We used the years 2001 and 2002 as pre-drought reference period to the drought year 2003, whereas the years 2004 and 2005 were

defined as post-drought period as recommended by Vitali et al. (2017). For the drought event 2018, we also used the previous two years as pre-drought reference to exclude the immediate effects of the heat wave of the summer in 2015 from the analysis (Muthers et al., 2017). For definition of post-drought years, only the tree-rings of the years 2019 and 2020 were available as increment cores in the three replications were sampled before the growing season 2021.

Besides tree-ring width (**trw**), we included mean tree-ring density ($\bar{\mathbf{d}}$), maximum latewood density (**mxld**) and stem radial biomass increment (**rbi**) in a multivariate analysis of resilience components and calculated the drought tolerance indices resistance (*Rt*), recovery (*Rc*) and resilience (*Rs*) as follows:

$$\begin{aligned} Rt_{i,j,k} &= \frac{Dr_{i,j,k}}{PreDr_{i,j,k}} \\ Rc_{i,j,k} &= \frac{PostDr_{i,j,k}}{Dr_{i,j,k}} \\ Rs_{i,j,k} &= \frac{PostDr_{i,j,k}}{PreDr_{i,j,k}} \end{aligned} \quad (2)$$

where *Dr* represents for the drought year *j* (2003 or 2018) the raw values of the measured variable *k* (**trw**, $\bar{\mathbf{d}}$, **mxld** or **rbi**) of tree *i*, whereas *PreDr* and *PostDr* denote the average values of the two pre-drought and two post-drought years, respectively. The raw data that were used to calculate the Lloret-indices for each variable are presented in **Supplementary Figures 2–5**.

The drought tolerance indices were tested for significant differences between species using bootstrapped *t*-tests for unpaired samples with 10,000 replications with a Satterthwaite approximation to the degrees of freedom (Efron and Tibshirani, 1993; Kohl, 2020). Bootstrapped *p*-values were adjusted using the false discovery rate to account for multiple inference (Benjamini and Hochberg, 1995). The same statistical procedure was used when testing for significant differences of raw measurements between tree species during the pre-drought, drought and post-drought years as the Lloret-indices only represent relative values and occlude different absolute growth levels. To test for significant differences of the Lloret-indices between the drought years 2003 and 2018, bootstrapped *t*-tests for paired samples were used to account for non-independence of repeated measurements. For visualization of all results, we calculated sample means with bias corrected and accelerated (bca) confidence intervals based on bootstrapping the sample mean 10,000 times.

To examine if drought tolerance indices of the investigated species varied with increasing elevation, we subsetted the data on the tree species level and formulated linear mixed-effects models with random intercepts as follows:

$$y_{i,j,k} = \beta_0 + \beta_1 E_{i,j,k} + b_j + b_{j,k} + e_{i,j,k} \quad (3)$$

where *y* represents the values of the response variable (*Rt*, *Rc*, or *Rs*) of tree *i* located within site *j* and transect *k*, β_0 is the intercept, $\beta_1 E$ denotes the fixed effect of the *z*-transformed elevation, b_j and $b_{j,k}$ are random effects on the site and transect level, whereas *e* denotes the residual error term. The linear mixed-effects models were fitted using the package *lme4* (Bates et al., 2015) and bootstrapped on the observational level with 10.000 replications followed by calculating the 95 %, 99 % and 99.9 % confidence interval (CI) of the bootstrapped coefficients. The drought tolerance indices were considered significant if at least 95 % of the bootstrapped β_0 coefficients were either above or below 1. The effect of elevation was considered significant if at least 95 % of the bootstrapped β_1 coefficients were either above or below 0. The effect of elevation was considered to vary significantly between tree species when at least 95 % of the differences between species-specific bootstrapped β_1 coefficients were either above or below 0. To account for multiple inference when testing between tree species, we used a Bonferroni correction to adjust the bootstrapped 95 % confidence interval ($CI_{adj} = 1 - 0.05 / 3$). In addition, we used the *MuMIn* package and quantified and averaged for all bootstrapped models the variance explained by the fixed effects ($R_M^2 = \text{Marginal } R^2$) and the variance explained by fixed and random effects combined ($R_C^2 = \text{Conditional } R^2$) (Barton, 2020).

As most years with intense reproductive effort might reduce the proportion of net primary production available for vegetative growth of trees, fructification is discussed as potential confounding factor influencing the results of the analysis of resilience components (Seifert and Müller-Starck, 2009; Hackett-Pain et al., 2017; Hirsch, 2019). For a better interpretation of the Lloret-indices and as complement to the inferential statistics described above, we used data of the forest monitoring program of the German province of Baden-Württemberg (Meining et al., 2020), which records the annual fructification intensity of individual forest trees in an 8 x 8 km sampling grid using an ordinal scale from 0 (absent) to 3 (abundant). For a robust assessment, we calculated for the time period 2001–2020 and the entire Black Forest study region for each of our conifer species the mean and mode of the annual fructification (i.e. coning) intensity (**Supplementary Figure 6**).

Results

Characterization of the growing conditions in the pre-drought, drought and post-drought years

Growing season air temperature averaged for the pre-drought years 2001 and 2002 and post-drought years 2004 and 2005 did not show any conspicuous anomalies. In June and August of the drought year 2003 distinct temperature anomalies occurred, and July temperature was above average

as well (Figure 2A). With the exception of April and May, no temperature anomalies were identified in the drought year 2018. However, monthly mean temperatures were generally above average during the complete growing season 2018 (Figure 2B). Negative precipitation anomalies were detected in June, August and September of 2003 and in July, September, October and November of 2018 (Figures 2C,D). In both drought years monthly precipitation sums were below average for the complete growing season. Monthly precipitation sum in July averaged for the post drought years 2019 and 2020 was also clearly below average (Figure 2D). The monthly climatic water balance showed negative anomalies in June and August 2003 as well as in July, September, October and November of 2018 (Figures 2E,F). The monthly climatic water balance in July averaged for the post-drought years 2019 and 2020 was clearly below average as well (Figure 2F). Relative plant available water in 2003 was below average during the whole growing season and distinct negative anomalies were detected between July and September (Figure 2G). Relative plant available water in 2018 was well below average in July and negative anomalies were increasing until November. For most of the growing season, the average conditions of the post-drought years 2019 and 2020 also showed plant available water below the long-term average, although distinct negative anomalies were not detected (Figure 2H).

During the 2001–2005 period all tree species, and in particular Norway spruce, showed the highest intensity of coning in the post-drought year 2004. Douglas fir showed stronger coning intensity than silver fir and Norway spruce in the pre-drought year 2016. During the time period 2001–2020, the highest mean coning intensities were documented in the drought year 2018 for all investigated tree species (Supplementary Figure 6).

Differences of drought tolerance indices between species and drought years

In this chapter we present the species-specific drought tolerance indices in respect to the drought events of 2003 and 2018, independent from elevation. All mentioned differences of the average values in the text below are significant between species and drought events ($p < 0.05$).

Mean tree-ring density (\bar{d}) of Norway spruce showed lower resistance to the 2003 drought compared to silver fir and Douglas fir, whereas in 2018 \bar{d} of both, silver fir and Norway spruce were reduced in comparison to Douglas fir. Resistance of \bar{d} of Norway spruce and silver fir was significantly lower in 2018 compared to 2003 (Figure 3A). Maximum latewood density (\mathbf{mxd}) of all species showed high resistance to the 2003 drought and even an increase in \mathbf{mxd} of silver fir in comparison to the other species was detected. Silver fir and Douglas fir also showed a substantial resistance of \mathbf{mxd} to the 2018 drought, whereas

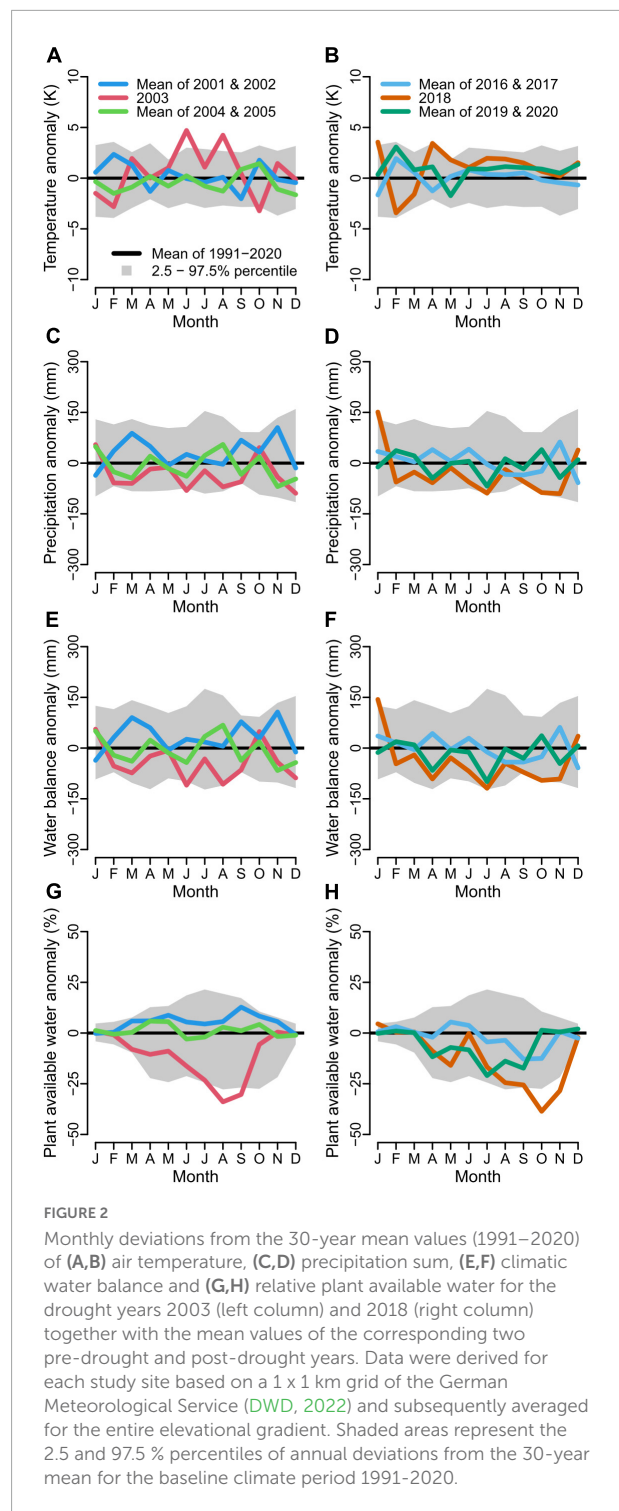


FIGURE 2

Monthly deviations from the 30-year mean values (1991–2020) of (A,B) air temperature, (C,D) precipitation sum, (E,F) climatic water balance and (G,H) relative plant available water for the drought years 2003 (left column) and 2018 (right column) together with the mean values of the corresponding two pre-drought and post-drought years. Data were derived for each study site based on a 1 x 1 km grid of the German Meteorological Service (DWD, 2022) and subsequently averaged for the entire elevational gradient. Shaded areas represent the 2.5 and 97.5 % percentiles of annual deviations from the 30-year mean for the baseline climate period 1991–2020.

\mathbf{mxd} of Norway spruce was significantly reduced in comparison. Resistance of \mathbf{mxd} of Norway spruce and silver fir was lower in 2018 compared to 2003, whereas no significant difference was documented for Douglas fir (Figure 3B). Tree-ring width (\mathbf{trw}) of Norway spruce showed lower resistance than silver fir and Douglas fir in 2003 and 2018. Silver fir and Douglas fir showed

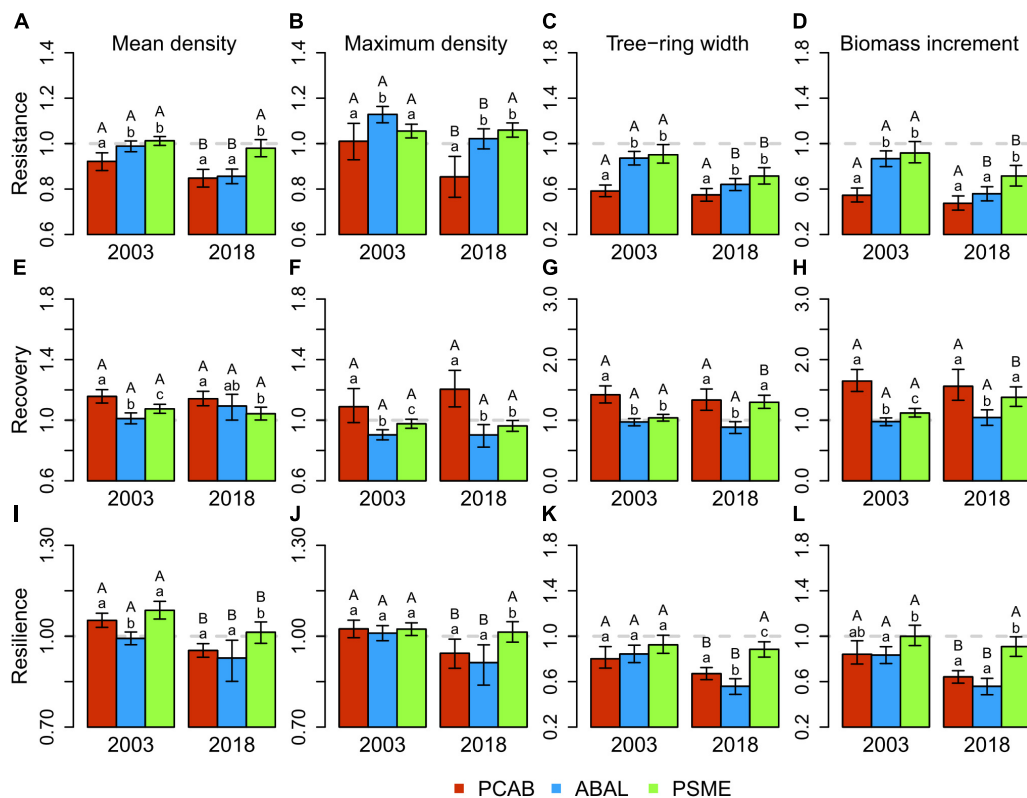


FIGURE 3

Resistance (A–D), recovery (E–H) and resilience (I–L) indices of mean tree-ring density, maximum latewood density, tree-ring width and stem radial biomass increment of Norway spruce (PCAB), silver fir (ABAL) and Douglas fir (PSME) for the two extreme drought events of the years 2003 and 2018. Error bars indicate bootstrapped 95% confidence intervals of the sample means based on 10,000 replications. Different lowercase letters above the error bars indicate significant differences between tree species within drought events. Different uppercase letters above the error bars indicate for each species significant differences between both drought events ($p < 0.05$).

lower resistance of \bar{trw} in 2018 compared to 2003, whereas the low resistance of Norway spruce did not differ significantly between the drought years (Figure 3C). Resistance patterns of stem radial biomass increment (\bar{rbi}) were quite similar in comparison to \bar{trw} , with the exception of the better resistance of \bar{rbi} of Douglas fir in comparison to silver fir in the year 2018 (Figure 3D).

Recovery of mean tree-ring density (\bar{d}) after the drought 2003 was higher in Norway spruce compared to Douglas fir, which in turn was higher than silver fir. Recovery of \bar{d} of Douglas fir after the 2018 drought event showed lower values in comparison to Norway spruce with no significant differences between silver fir and Douglas fir. No significant differences between drought events were detected for any of the investigated species (Figure 3E). Recovery of maximum latewood density (\bar{mxd}) after the 2003 drought event was higher in Norway spruce compared to Douglas fir, which showed better recovery than silver fir. Recovery of \bar{mxd} after the 2018 drought was lower in silver fir and Douglas fir compared to Norway spruce. No differences in recovery of \bar{mxd} were detected between drought years for any tree species (Figure 3F). Tree-ring width (\bar{trw}) of

Norway spruce showed higher recovery values than silver fir and Douglas fir after the 2003 drought. After the drought of 2018, recovery values of \bar{trw} of silver fir were lower also in comparison to Norway spruce and Douglas fir. Douglas fir showed a better recovery after 2018 in comparison to the post-drought years of 2003 (Figure 3G). Recovery patterns were similar for stem radial biomass increment (\bar{rbi}) and \bar{trw} . However, recovery values of Douglas fir \bar{rbi} were higher than silver fir after 2003 and after 2018 (Figure 3H).

Resilience of mean tree-ring density (\bar{d}) of Norway spruce and Douglas fir after the 2003 drought reached higher values in comparison to silver fir. Douglas fir showed higher resilience compared to silver fir and Norway spruce after the drought of 2018. All species showed lower resilience after 2018 compared to the resilience after 2003 (Figure 3I). No differences between species were detected regarding resilience of maximum latewood density (\bar{mxd}) after the 2003 drought. In contrast, Douglas fir showed higher resilience values after the 2018 drought compared to Norway spruce and silver fir, who both also showed lower resilience in 2018 compared to 2003 (Figure 3J). No differences in the resilience of tree-ring width

(**trw**) were detected between species after the drought in 2003. However, Douglas fir showed higher resilience of **trw** compared to Norway spruce after 2018, whose resilience was also higher in comparison to silver fir (Figure 3K). Resilience of stem radial biomass increment (**rbi**) showed similar patterns as **trw** with the exception that Douglas fir showed a higher resilience than silver fir after 2003 and that no differences between silver fir and Norway spruce were detected after 2018 (Figure 3L).

Effects of elevation on drought tolerance indices

This chapter describes the effects of elevation on the drought tolerance indices of the investigated species for the 2003 and 2018 drought events. All mentioned elevational trends (i.e., β_1 coefficients) or differences in elevational trends between species were significantly different from zero based on bootstrapped 95% confidence intervals.

Resistance of mean tree-ring density (\bar{d}) increased significantly with elevation for silver fir in 2003 and 2018 and for Douglas fir in 2018 (Figures 4A,B and Supplementary Table 1). Recovery values of \bar{d} were significantly increased at lower elevations for silver fir after 2003 and for silver fir and Norway spruce after 2018 (Figures 4C,D), whereas silver fir also showed higher resilience of \bar{d} at lower elevations after the 2003 drought (Figures 4E,F). Elevational trends of the resistance and recovery of \bar{d} were significantly different between Norway spruce and silver fir (Figures 4A,C and Supplementary Table 2), whereas elevational response of recovery values of \bar{d} between Douglas fir and silver fir was significantly different in respect to the 2003 drought event (Figure 4C).

No significant effects of elevation on the resistance, recovery and resilience of maximum latewood density (**mxd**) were detected for Norway spruce and Douglas fir (Figures 5A–F and Supplementary Table 3). Silver fir showed lower resistance with decreasing elevation in 2018 (Figure 5B), but also considerable recovery of **mxd** during the post-drought years at the same sites (Figure 5D). Silver fir showed also increased resilience of **mxd** with increasing elevation in 2003 (Figure 5E).

Resistance of stem radial biomass increment (**rbi**) increased significantly with higher elevation for silver fir in 2003 and 2018 and for Norway spruce fir in 2018 (Figures 6A,B and Supplementary Table 4). Increased recovery values of **rbi** were detected at lower elevations for silver fir and Douglas fir after the 2003 drought and for silver fir and Norway spruce after the 2018 drought (Figures 6C,D). Silver fir showed increased resilience of **rbi** with increasing elevation after the drought in 2003 (Figure 6E). However, no significant effects of elevation on resilience of **rbi** were detected after the drought in 2018 (Figure 6F). Elevational trends of the resistance of **rbi** were significantly different between Norway spruce and silver fir in 2003 (Figure 6A and Supplementary Table 2). Significant differences of the elevational response of the recovery of **rbi** after

2018 were also detected between Douglas fir and Norway spruce (Figure 6D). The effect of elevation on the resilience of **rbi** after 2003 was also significantly different between Douglas fir and silver fir (Figure 6E). Elevational trends and significance levels of drought tolerance indices of tree-ring width mostly pointed into similar directions as with **rbi** (Supplementary Figure 7 and Supplementary Table 5).

Growth rates and wood density before, during, and after drought years

Douglas fir constantly showed the highest values of mean tree-ring density (\bar{d}), whereas silver fir showed higher \bar{d} than Norway spruce only during the pre-drought and drought of 2003 (Supplementary Figures 8A–C). Douglas fir showed higher values of maximum latewood density (**mxd**) than silver fir during the pre-drought of 2003 and post-droughts of 2003 and 2018 as well as higher values of **mxd** than Norway spruce during the 2018 drought. Norway spruce showed higher **mxd** values than silver fir during pre-drought and post-drought years of 2003 and 2018 (Supplementary Figures 8D–F). Norway spruce showed in most cases significantly lower levels of tree-ring width (**trw**) and radial biomass increment (**rbi**) compared to silver fir and Douglas fir (Supplementary Figures 8G–I). Silver fir and Douglas fir showed competitive levels of **trw** and **rbi** during the pre-drought, drought and post-drought years of 2003, whereas for the time period around 2018, growth levels of silver fir dropped much closer to Norway spruce.

Discussion

Several studies reported higher resistance and resilience of secondary growth of silver fir and Douglas fir to the extreme drought event of 2003 in comparison to Norway spruce (van der Maaten-Theunissen, 2012; Uhl et al., 2013; Vitali et al., 2017). The high drought sensitivity of Norway spruce is often attributed to the limited potential of its shallow root system to access water reserves located in deeper soil layers during extensive drought periods (Vitali et al., 2017). Norway spruce originates mainly from mountainous, subalpine and boreal regions, but was frequently planted in the Black Forest region on sites outside its natural distribution, where it is maladapted and located far beyond its ecological optimum (Schmidt-Vogt, 1987). In contrast, silver fir is generally recognized as an integral component of the potential natural vegetation of large parts of the Black Forest region (Konnerth and Bergmann, 1995; Kohnle et al., 2011). On well drained soils, its taproot system has the potential to exploit deeper soil water reserves, thus enabling silver fir to endure longer drought periods better than Norway spruce (Aussenac, 2002; Vitasse et al., 2019). It is also suggested that silver fir was widely distributed during warm periods of paleoclimates and its current

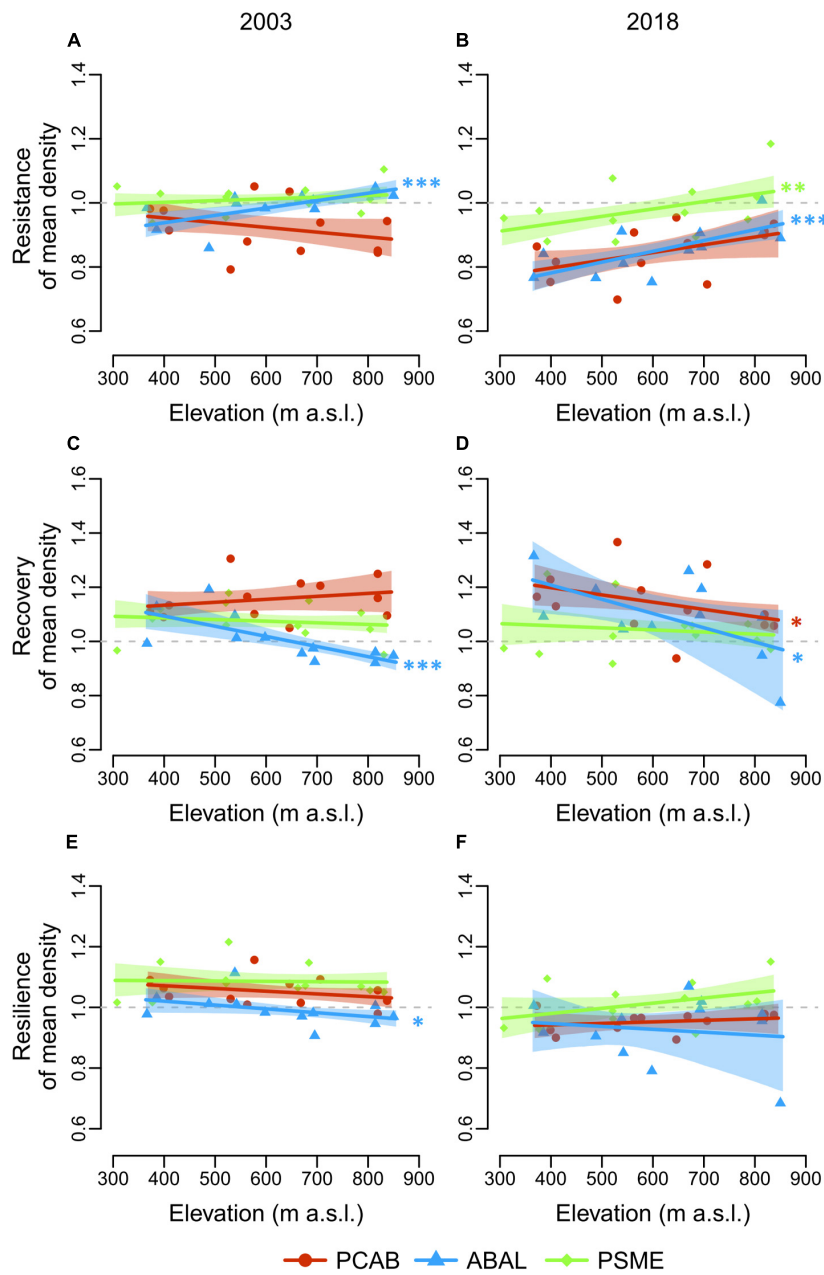


FIGURE 4

Resistance (A,B), recovery (C,D) and resilience (E,F) indices of mean tree-ring density of Norway spruce (PCAB), silver fir (ABAL) and Douglas fir (PSME) in response to elevation for the two extreme drought events of the years 2003 (left) and 2018 (right). Transparent ribbons indicate bootstrapped 95 % confidence intervals of predictions of linear mixed-effects models based on 10,000 replications. For illustration, data points were averaged on the stand level. Asterisks on the right side of the panels indicate if slopes of the regression lines are significantly different from zero based on bootstrapped confidence intervals: 95% "*", 99% "**", 99.9% "***", 99.9% "****". Marginal R^2 and conditional R^2 of the linear mixed-effects models are listed in [Supplementary Table 1](#).

distribution range partly also includes Mediterranean sites (Aussenac, 2002; Vitasse et al., 2019). Due to its potentially lower drought sensitivity and presumably more positive responses to global warming, Vitali et al. (2018) recently projected net increases of tree-ring growth of silver fir until the end of the 21st century while largely outperforming Norway spruce and even Douglas fir.

Indeed, our hypotheses that Norway spruce would show a more severe and negative growth response than silver fir and Douglas fir was partly confirmed by its low resistance indices for the 2003 drought year. Here, tree-ring width (*trw*), radial biomass increment (*rbi*), mean tree-ring density (\bar{d}) and maximum latewood density (*mxld*) of silver fir and Douglas fir showed almost exclusively higher values compared to Norway

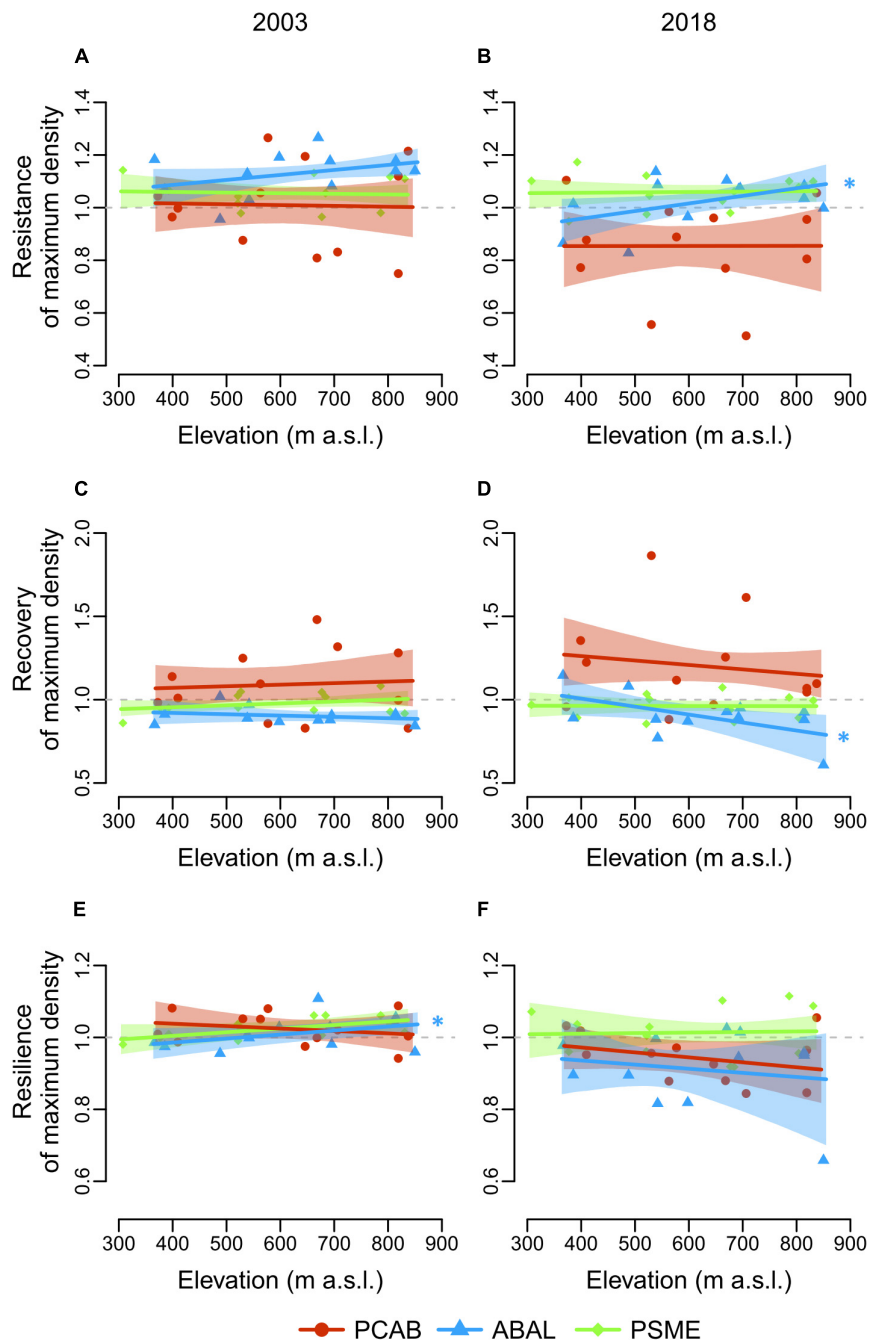


FIGURE 5

Resistance (A,B), recovery (C,D) and resilience (E,F) indices of maximum latewood density of Norway spruce (PCAB), silver fir (ABAL) and Douglas fir (PSME) in response to elevation for the two extreme drought events of the years 2003 (left) and 2018 (right). Transparent ribbons indicate bootstrapped 95 % confidence intervals of predictions of linear mixed-effects models based on 10,000 replications. For illustration, data points were averaged on the stand level. Asterisks on the right side of the panels indicate if slopes of the regression lines are significantly different from zero based on bootstrapped confidence intervals: 95% **, 99% ***, 99.9% ****. Marginal R² and conditional R² of the linear mixed-effects models are listed in [Supplementary Table 3](#).

spruce, which corresponds to results of previous studies in the Black Forest region (Vitali et al., 2017). Also, in 2018 we detected higher resistance of **trw** of silver fir in comparison to Norway spruce, but we could not substantiate these findings for \bar{d} or **rbi**. In addition, \bar{d} of Norway spruce and silver

fir, **mxd** of Norway spruce as well as **trw** and **rbi** of silver fir and Douglas fir showed considerably lower resistance in 2018 compared to 2003. The strong decrease of resistance indices of silver fir in 2018 compared to 2003 is in agreement with previous findings of low drought resistance, impaired

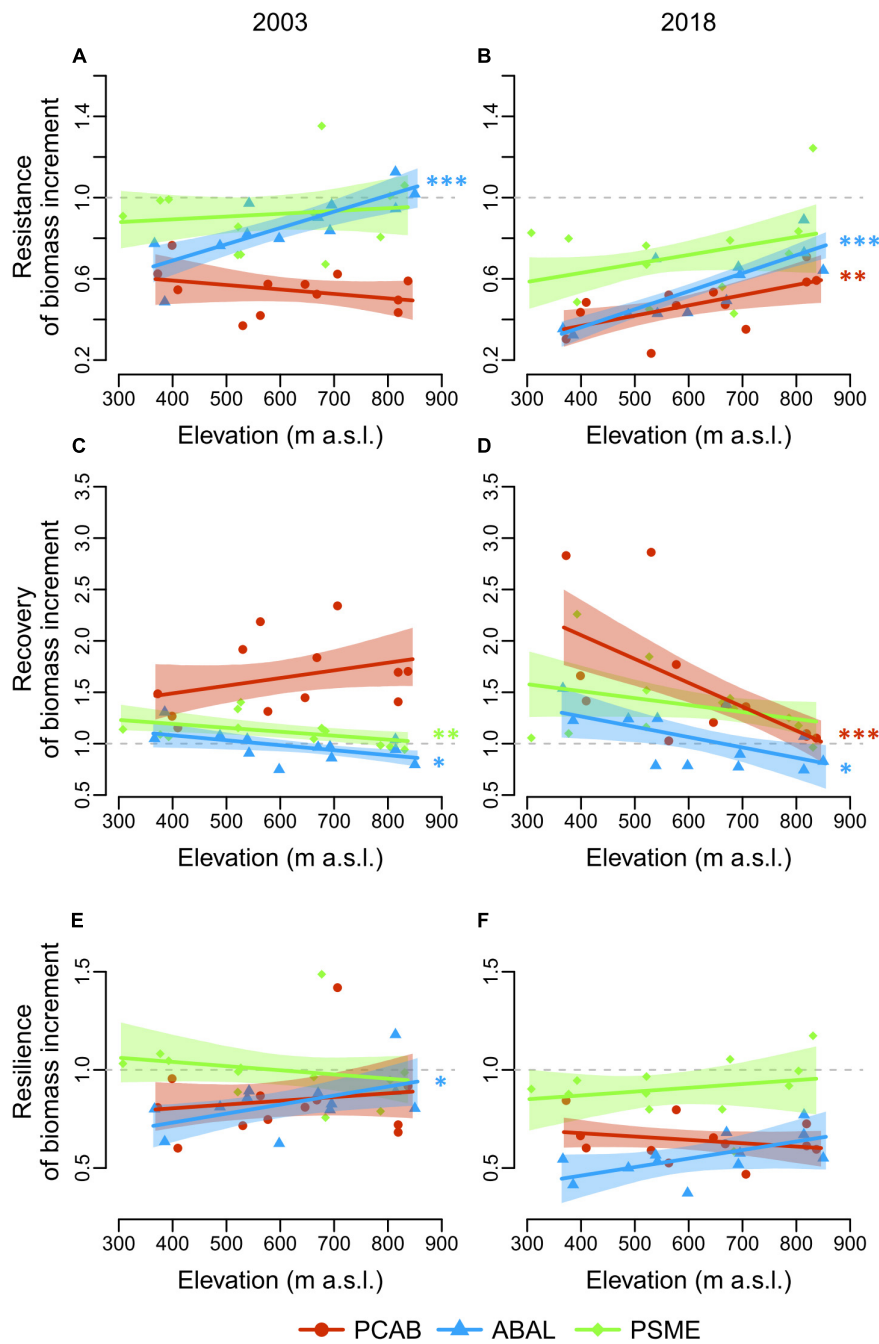


FIGURE 6

Resistance (A,B), recovery (C,D) and resilience (E,F) indices of stem radial biomass increment of Norway spruce (PCAB), silver fir (ABAL) and Douglas fir (PSME) in response to elevation for the two extreme drought events of the years 2003 (left) and 2018 (right). Transparent ribbons indicate bootstrapped 95% confidence intervals of predictions of linear mixed-effects models based on 10,000 replications. For illustration, data points were averaged on the stand level. Asterisks on the right side of the panels indicate if slopes of the regression lines are significantly different from zero based on bootstrapped confidence intervals: 95% **, 99% ***, 99.9% ****. Marginal R^2 and conditional R^2 of the linear mixed-effects models are listed in [Supplementary Table 4](#).

xylem cell differentiation processes and reduced woody biomass production in the study region during 2018 (Larysch et al., 2021, 2022). In agreement with previous findings with respect to the 2003 drought (Vitali et al., 2017), we could also substantiate higher drought resistance of \bar{d} , \bar{trw} , and \bar{rbi} of

silver fir in 2018 with increasing elevation. However, it must be noted that resistance was considerably more reduced at high elevation sites in 2018 compared to 2003. Norway spruce also showed increased drought resistance of \bar{trw} and \bar{rbi} with increasing elevation in 2018. Nevertheless, resistance values

were considerably reduced across the entire elevational gradient, which is consistent with previous conclusions of high drought sensitivity and low climatic stability of Norway spruce even at high elevation sites in the Black Forest region (van der Maaten-Theunissen et al., 2013; Vitali et al., 2017).

A possible explanation of the decreased drought resistance of all species in 2018 might be the high coning intensity in the same year of all investigated species, which likely had caused substantial reallocations of carbohydrates due to the sink strength of cone production while simultaneously decreasing the proportion of net primary production available for vegetative growth of trees (van der Maaten-Theunissen, 2012; Hackett-Pain et al., 2017; Hirsch, 2019). In contrast, Seifert and Müller-Starck (2009) did not detect trade-offs between cone production and vegetative growth of Norway spruce during and after mast years. This is partly confirmed by our results for Norway spruce, which did not show a lower resistance of **trw** and **rbi** in the mast year 2018 compared to 2003. Besides the fact that resistance indices of **trw** and **rbi** of Norway spruce were the lowest in both drought years, the lower resistance of \bar{d} and **mxd** of spruce in 2018 compared to 2003 indicates that resource availability for latewood production was considerably compromised by the multiple stressors of cone production, water deficit, depleted carbohydrate reserves and increased respiratory demands during the extreme summer drought of 2018 (Teskey et al., 2015; Hackett-Pain et al., 2017; Arend et al., 2021). Previous studies have shown that the rate of cell wall thickening of conifers was significantly reduced during periods of intra-seasonal drought, but endogenous control can potentially compensate reduced cell differentiation rates by prolonging their duration (Balducci et al., 2016; Stangler et al., 2021; Larysch et al., 2022). We hypothesize that such compensatory mechanisms became ineffective during latewood formation of 2018 and that drought stress in late summer and autumn might have caused a premature cessation of xylem cell differentiation phases (Gruber et al., 2010; Saderi et al., 2019; Larysch et al., 2021). In addition, the temporal development of drought conditions followed slightly different patterns in the years 2003 and 2018. Consequently, latewood formation in 2018 might have been more compromised by drought as in this year the most extreme anomalies of soil moisture deficits were detected during autumn (Figure 2H), which is the time where cell wall thickening and lignification of the last latewood cells of the investigated species in the study region can be expected (Miller et al., 2022).

Recovery of **trw** and **rbi** after the 2003 drought was higher in Norway spruce compared to silver fir and Douglas fir, which is only partly in agreement with previous research identifying no differences in recovery between spruce and Douglas fir (Vitali et al., 2017). Recovery of silver fir was lower after both drought years and for almost all investigated variables in comparison to Norway spruce. In contrast to 2003, the low recovery after the 2018 drought eventually resulted also in significant reductions

of the resilience indices of silver fir for all investigated growth variables. Our findings document the inability of silver fir to fully recover from the 2018 drought as well as the significantly lower resilience of all investigated variables of silver fir and Norway spruce in the post-drought years of 2018 compared to the post-drought years of 2003. Contrary to the resilience patterns after 2003, we also could not identify improved resilience of **trw** and **rbi** of silver fir with increasing elevation in 2018, but even lower resilience values compared to Norway spruce at low elevation sites. These results largely falsify our hypothesis and challenge previous findings and generalized conjectures of the potentially lower drought sensitivity of silver fir in comparison to Norway spruce based on the drought of 2003 (Uhl et al., 2013; van der Maaten-Theunissen et al., 2013; Vitali et al., 2017). Our results also correspond closely with the assessment of the effects of the extreme drought of 2018 on forest ecosystems in Austria, Germany and Switzerland by Schuldt et al. (2020), who documented legacy-effects with severe impairment of the physiological recovery as well as unexpected mortality of silver fir even on less drought-prone sites. This suggests that the findings of our study might also apply beyond the stands and study region we have investigated. The decline in vitality of silver fir was also reflected by missing tree-rings and impending decline of four of our sample trees after the 2018 drought, a phenomenon which was not constrained to low elevations and generally not detected for Norway spruce or Douglas fir (Supplementary Figure 4).

Another possible explanation for the weak resilience and recovery of silver fir after the 2018 drought could be its inability to fully recover when post-drought years include below average water availability and transient drought conditions as well (Figure 2). A possible solution would be to combine several years into a single drought event (Schwarz et al., 2020), which was not feasible in our study as the increment cores were sampled already 2 years after the 2018 drought. To maintain comparability with previous research in the study region (Vitali et al., 2017), we also stayed close to the original concept of drought tolerance indices (Lloret et al., 2011), although methodological innovations when calculating such indices should be considered in future studies (Schwarz et al., 2020). Independent of these considerations, Douglas fir showed generally the highest resilience for all investigated variables following the 2018 drought. Therefore, in agreement with our hypotheses, our results confirm the superior capacity of Douglas fir to absorb drought stress periods while maintaining high levels of productivity, wood density and carbon sequestration across all elevations (Eilmann and Rigling, 2012; Vitali et al., 2017).

Conclusion

This study presented a multivariate analysis of resilience components in respect to the extreme drought years 2003 and

2018. As expected, our results for Norway spruce corroborate projections of its ongoing decline during climate change as the reductions of wood density and biomass production indicated high drought sensitivity at all elevations. Moreover, resilience indices of mean tree-ring density, maximum latewood density, tree-ring width and biomass production were even lower after the drought of 2018 compared to the previous drought of 2003. Silver fir, a potential substitute tree species for Norway spruce, showed unexpected results with resistance and resilience indices being significantly lower in 2018 compared to 2003. We conclude that silver fir might be more vulnerable to drought than previously expected, especially at low elevations. Silver fir might also be increasingly susceptible to the effects of climate change if drought events coincide with fructification years and if post-drought years include periods of transient water stress as well. Future research should explore the potentially non-linear growth responses of silver fir to the effects of temperature and water availability. We speculate that the tipping point from positive to negative impacts of global warming on productivity of silver fir might be reached earlier than previously projected. In contrast, superiority in growth rates and growth resilience of Douglas fir was especially pronounced during the drought of 2018, even though high coning intensity was present for all investigated tree species as a possible confounding factor to exacerbate the drought stress effects in the study region.

Data availability statement

The raw measurements used for data analysis can be made available by the authors upon reasonable request.

Author contributions

DS wrote the manuscript with support from TM, EL, HH, TS, HP, and H-PK. H-PK, EL, and DS conceptualized the study. TM, HH, and DS done the field work. DS conducted the measurements of tree-ring width and wood density. DS performed the final data analysis with suggestions of H-PK, TS, and HP. All authors contributed to the article and approved the submitted version.

References

- Arend, M., Link, R. M., Patthey, R., Hoch, G., Schuldt, B., and Kahmen, A. (2021). Rapid hydraulic collapse as cause of drought-induced mortality in conifers. *Proc. Natl. Acad. Sci. U.S.A.* 118:e2025251118. doi: 10.1073/pnas.2025251118
- Aussenac, G. (2002). Ecology and ecophysiology of circum-Mediterranean firs in the context of climate change. *Ann. For. Sci.* 59, 823–832. doi: 10.1051/forest/2002080

Funding

This work was supported by the German Federal Ministry of Food and Agriculture and the German Federal Ministry for the Environment, Nature Conservation and Nuclear Safety with grants: 22W-K-4-148. We acknowledge support by the Open Access Publication Fund of the University of Freiburg.

Acknowledgments

We thank Clemens Koch, Melchior Schliephack, Robert Linne, Kristin Bondza, and Lea Kopp for technical support during field and laboratory work. We are grateful to the local forest administration to facilitate our field work activities. We also thank all reviewers of this manuscript for their helpful comments and valuable suggestions.

Conflict of interest

The authors declare that the research was conducted in the absence of any commercial or financial relationships that could be construed as a potential conflict of interest.

Publisher's note

All claims expressed in this article are solely those of the authors and do not necessarily represent those of their affiliated organizations, or those of the publisher, the editors and the reviewers. Any product that may be evaluated in this article, or claim that may be made by its manufacturer, is not guaranteed or endorsed by the publisher.

Supplementary material

The Supplementary Material for this article can be found online at: <https://www.frontiersin.org/articles/10.3389/fevo.2022.907492/full#supplementary-material>

- Balducci, L., Cuny, H. E., Rathgeber, C. B. K., Deslauriers, A., Giovannelli, A., and Rossi, S. (2016). Compensatory mechanisms mitigate the effect of warming and drought on wood formation. *Plant Cell. Environ.* 39, 1338–1352. doi: 10.1111/pce.12689

Barton, K. (2020). *MuMIn: Multi-model inference*. Available online at: <https://CRAN.R-project.org/package=MuMIn> (accessed July 18, 2022).

- Bates, D., Mächler, M., Bolker, B., and Walker, S. (2015). Fitting linear mixed-effects models using lme4. *J. Stat. Soft.* 67, 1–48. doi: 10.18637/jss.v067.i01
- Benjamini, Y., and Hochberg, Y. (1995). Controlling the false discovery rate: A practical and powerful approach to multiple testing. *J. R. Statist. Soc. B* 57, 289–300. doi: 10.1111/j.2517-6161.1995.tb02031.x
- BMEL (2014). *Dritte Bundeswaldinventur - Ergebnisdatenbank*. Available online at: <https://bwi.info/> (accessed February 23, 2022).
- Bolte, A., Ammer, C., Löf, M., Madsen, P., Nabuurs, G. J., Schall, P., et al. (2009). Adaptive forest management in central Europe: Climate change impacts, strategies and integrative concept. *Scand. J. For. Res.* 24, 473–482. doi: 10.1080/02827580903418224
- Brandl, S., Paul, C., Knoke, T., and Falk, W. (2020). The influence of climate and management on survival probability for Germany's most important tree species. *Forest Ecol. Manag.* 458:117652. doi: 10.1016/j.foreco.2019.117652
- Büntgen, U., Frank, D. C., Kaczka, R. J., Verstege, A., Zwijacz-Kozica, T., and Esper, J. (2007). Growth responses to climate in a multi-species tree-ring network in the Western Carpathian Tatra Mountains, Poland and Slovakia. *Tree Physiol.* 27, 689–702. doi: 10.1093/treephys/27.5.689
- Conkey, L. E. (1979). Response of tree-ring density to climate in Maine, U.S.A. *Tree-ring Bull.* 39, 29–38.
- Diaconu, D., Kahle, H. P., and Spiecker, H. (2017). Thinning increases drought tolerance of European beech: A case study on two forested slopes on opposite sides of a valley. *Eur. J. For. Res.* 19:1188. doi: 10.1007/s10342-017-1033-8
- Dietrich, H., Wolf, T., Kawohl, T., Wehberg, J., Kändler, G., Mette, T., et al. (2019). Temporal and spatial high-resolution climate data from 1961 to 2100 for the German National Forest Inventory (NFI). *Ann. For. Sci.* 76:171. doi: 10.1007/s13595-018-0788-5
- DWD (2022). *DWD Climate Data Center (CDC): Grids of monthly averaged daily air temperature (2m), total precipitation, accumulated potential evapotranspiration over grass and soil moisture under grass and sandy loam over Germany*. Available online at: https://opendata.dwd.de/climate_environment/CDC/grids_germany/monthly/ (accessed July 29, 2022).
- Efron, B., and Tibshirani, R. J. (1993). *An introduction to the bootstrap*. Boston, MA: Springer US.
- Eilmann, B., and Rigling, A. (2012). Tree-growth analyses to estimate tree species' drought tolerance. *Tree Physiol.* 32, 178–187. doi: 10.1093/treephys/tps004
- Gruber, A., Strobl, S., Veit, B., and Oberhuber, W. (2010). Impact of drought on the temporal dynamics of wood formation in *Pinus sylvestris*. *Tree Physiol.* 30, 490–501. doi: 10.1093/treephys/tpq003
- Hackett-Pain, A. J., Lageard, J. G. A., and Thomas, P. A. (2017). Drought and reproductive effort interact to control growth of a temperate broadleaved tree species (*Fagus sylvatica*). *Tree Physiol.* 37, 744–754. doi: 10.1093/treephys/tpx025
- Hartl-Meier, C., Dittmar, C., Zang, C., and Rothe, A. (2014). Mountain forest growth response to climate change in the Northern Limestone Alps. *Trees* 28, 819–829. doi: 10.1007/s00468-014-0994-1
- Henin, J.-M., Pollet, C., Schmitt, U., Blohm, J.-H., Koch, G., Melcher, E., et al. (2019). "Technological properties of Douglas-fir wood," in *Douglas-fir: An option for Europe*, eds H. Spiecker, M. Lindner, and J. K. Schuler (Joensuu: European Forest Institute), 89–97.
- Hirsch, M. (2019). *Das Stammdickenwachstum von Buchen und Tannen in Baden-Württemberg unter dem Einfluss von Witterung und Klimaveränderungen – Langfristige Trends und kurzfristige Reaktionen auf Trockenheit*. PhD thesis. Freiburg: Albert-Ludwigs-Universität Freiburg.
- Kahle, H. P. (2006). "Impact of the drought in 2003 on intra- and inter-annual stem radial growth of beech and spruce along an altitudinal gradient," in *TRACE - Tree rings in archaeology, climatology and ecology, volume 4: Proceedings of the Dendrosymposium 2005, April 21st - 23rd 2005, Fribourg, Switzerland*, eds I. Heinrich, H. Gärtner, M. Monbaron, and G. H. Schleser (Jülich: Forschungszentrum Jülich), 151–163.
- Knibbe, B. (2004). *PAST4 Q19 – Personal analysis system for tree ring research: Instruction manual, SCIE/Bernhard Knibbe, Version 4. Vienna*.
- Kohl, M. (2020). *MKinfer: Inferential statistics*. Available online at: <http://www.stamats.de> (Accessed February 23, 2022).
- Kohnle, U., Klädtke, J., and Chopard, B. (2019). "Management of douglas-fir," in *Douglas-fir: An option for Europe*, eds H. Spiecker, M. Lindner, and J. K. Schuler (Joensuu: European Forest Institute), 73–83.
- Kohnle, U., Yue, C., and Cullmann, D. (2011). "Wachstum der Weißtanne in Südwestdeutschland: Entwicklung, Klima-Risiko und Verjüngung," in *Wälder im Klimawandel – Weißtanne und Küstentanne*, ed. Bayerische Landesanstalt für Wald und Forstwirtschaft (LWF) (Freising: Bayerische Landesanstalt für Wald und Forstwirtschaft), 41–50.
- Konnert, M., and Bergmann, F. (1995). The geographical distribution of genetic variation of silver fir (*Abies alba*, Pinaceae) in relation to its migration history. *Pl. Syst. Evol.* 196, 19–30. doi: 10.1007/BF00985333
- Lamlom, S. H., and Savidge, R. A. (2003). A reassessment of carbon content in wood: Variation within and between 41 North American species. *Biomass Bioenergy* 25, 381–388. doi: 10.1016/S0961-9534(03)00033-3
- Larysch, E., Stangler, D. F., Nazari, M., Seifert, T., and Kahle, H.-P. (2021). Xylem phenology and growth response of European beech, silver fir and Scots pine along an elevational gradient during the extreme drought year 2018. *Forests* 12:75. doi: 10.3390/f12010075
- Larysch, E., Stangler, D. F., Puhlmann, H., Rathgeber, C. B. K., Seifert, T., and Kahle, H.-P. (2022). The 2018 hot drought pushed conifer wood formation to the limit of its plasticity: Consequences for woody biomass production and tree ring structure. *Plant Biol.* [Online ahead of print]. doi: 10.1111/plb.13399
- Leskinen, P., Cardellini, G., González-García, S., Hurmekoski, E., Sathre, R., Seppälä, J., et al. (2018). *Substitution effects of wood-based products in climate change mitigation*. Joensuu: EFI.
- Lloret, F., Keeling, E. G., and Sala, A. (2011). Components of tree resilience: Effects of successive low-growth episodes in old ponderosa pine forests. *Oikos* 120, 1909–1920. doi: 10.1111/j.1600-0706.2011.19372.x
- Luss, S., Lundqvist, S.-O., Evans, R., Grah, T., Olsson, L., Petit, G., et al. (2019). Within-ring variability of wood structure and its relationship to drought sensitivity in Norway spruce trunks. *IAWA J.* 40, 288–310. doi: 10.1163/22941932-40190216
- Maringer, J., Stelzer, A.-S., Paul, C., and Albrecht, A. (2021). Ninety-five years of observed disturbance-based tree mortality modeled with climate-sensitive accelerated failure time models. *Eur. J. For. Res.* 140, 255–272. doi: 10.1007/s10342-020-01328-x
- Martinez-Meier, A., Sanchez, L., Pastorino, M., Gallo, L., and Rozenberg, P. (2008). What is hot in tree rings? The wood density of surviving Douglas-firs to the 2003 drought and heat wave. *Forest Ecol. Manag.* 256, 837–843. doi: 10.1016/j.foreco.2008.05.041
- Meining, S., Puhlmann, H., Hartmann, P., Hallas, T., Hoch, R., and Augustin, N. (2020). *Waldzustandsbericht 2020*. Freiburg: Forstliche Versuchs- und Forschungsanstalt Baden-Württemberg (FVA).
- Miller, T. W., Stangler, D. F., Larysch, E., Honer, H., Seifert, T., Puhlmann, H., et al. (2022). Longer and faster: Intra-annual growth dynamics of Douglas fir outperform Norway spruce and silver fir over wide climatic gradients. *Agr. Forest Meteorol.* 321:108970. doi: 10.1016/j.agrformet.2022.108970
- Montwé, D., Spiecker, H., and Hamann, A. (2015). Five decades of growth in a genetic field trial of Douglas-fir reveal trade-offs between productivity and drought tolerance. *Tree Genet. Genomes* 11:29. doi: 10.1007/s11295-015-0854-1
- Muthers, S., Laschewski, G., and Matzarakis, A. (2017). The summers 2003 and 2015 in South-West Germany: Heat waves and heat-related mortality in the context of climate change. *Atmosphere* 8:224. doi: 10.3390/atmos8110224
- R Core Team (2022). *R: A language and environment for statistical computing*. Vienna: R Core Team.
- Rosner, S., Světlík, J., Andreassen, K., Børja, I., Dalsgaard, L., Evans, R., et al. (2014). Wood density as a screening trait for drought sensitivity in Norway spruce. *Can. J. For. Res.* 44, 154–161. doi: 10.1139/cjfr-2013-0209
- Saderi, S., Rathgeber, C. B. K., Rozenberg, P., and Fournier, M. (2019). Phenology of wood formation in larch (*Larix decidua* Mill.) trees growing along a 1000-m elevation gradient in the French Southern Alps. *Ann. For. Sci.* 76:214. doi: 10.1007/s13595-019-0866-3
- San-Miguel-Ayaz, J., Rigo, D., Caudullo, G., Houston Durrant, T., and Mauri, A. (eds) (2016). *European atlas of forest tree species*. Luxembourg: Publications Office of the European Union.
- Schinker, M. G., Hansen, N., and Spiecker, H. (2003). High-Frequency densitometry - a new method for the rapid evaluation of wood density variations. *IAWA J.* 24, 231–239. doi: 10.1163/22941932-90001592
- Schmidt-Vogt, H. (1987). *Die Fichte: Ein handbuch in 2 bänden*. Hamburg: Parey.
- Schmied, G., Hilmers, T., Uhl, E., and Pretzsch, H. (2022). The past matters: Previous management strategies modulate current growth and drought responses of Norway spruce (*Picea abies* H. Karst.). *Forests* 13:243. doi: 10.3390/f13020243
- Schuld, B., Buras, A., Arend, M., Vitasse, Y., Beierkuhnlein, C., Damm, A., et al. (2020). A first assessment of the impact of the extreme 2018 summer drought on Central European forests. *Basic Appl. Ecol.* 45, 86–103. doi: 10.1016/j.baee.2020.04.003

- Schwarz, J., Skiadaresis, G., Kohler, M., Kunz, J., Schnabel, F., Vitali, V., et al. (2020). Quantifying growth responses of trees to drought—a critique of commonly used resilience indices and recommendations for futures studies. *Curr. Forestry Rep.* 6, 185–200. doi: 10.1007/s40725-020-00119-2
- Seifert, T., and Müller-Starck, G. (2009). Impacts of fructification on biomass production and correlated genetic effects in Norway spruce (*Picea abies* [L.] Karst.). *Eur. J. For. Res.* 128, 155–169. doi: 10.1007/s10342-008-0219-5
- Spiecker, H., Lindner, M., and Schuler, J. K. (eds) (2019). *Douglas-fir: An option for Europe*. Joensuu: European Forest Institute.
- Spiecker, H., Schinker, M. G., Hansen, J., Park, Y. I., Ebding, T., and Doll, W. (2000). Cell structure in tree rings: Novel methods for preparation and image analysis of large cross sections. *IAWA J.* 21, 361–373. doi: 10.1163/22941932-90000253
- Sprengel, L., Cheng, Z., Hipler, S.-M., Wu, S., and Spiecker, H. (2020). Mean annual wood density variations of *Larix gmelinii* (Rupr.), *Quercus mongolica* Fisch. ex Ledeb., and *Pinus tabulaeformis* Carr. at two different stem heights. *Forests* 11:394. doi: 10.3390/f11040394
- Stangler, D. F., Kahle, H.-P., Raden, M., Larysch, E., Seifert, T., and Spiecker, H. (2021). Effects of intra-seasonal drought on kinetics of tracheid differentiation and seasonal growth dynamics of Norway spruce along an elevational gradient. *Forests* 12:274. doi: 10.3390/f12030274
- Teskey, R., Wertin, T., Bauweraerts, I., Ameye, M., McGuire, M. A., and Steppe, K. (2015). Responses of tree species to heat waves and extreme heat events. *Plant Cell. Environ.* 38, 1699–1712. doi: 10.1111/pce.12417
- Thomas, S. C., and Martin, A. R. (2012). Carbon content of tree tissues: A synthesis. *Forests* 3, 332–352. doi: 10.3390/f3020332
- Uhl, E., Ammer, C., Spellmann, H., Schölch, M., and Pretzsch, H. (2013). Zuwachstrend und Stressresilienz von Tanne und Fichte im Vergleich. *Allg. Forst Jagdztg.* 184, 278–292.
- van der Maaten-Theunissen, M. J. (2012). “Climate response of radial growth of silver fir (*Abies alba* Mill.) and Norway spruce (*Picea abies* (L.) Karst.) in the Black Forest, Germany,” in *TRACE - Tree rings in archaeology, climatology and ecology, volume 10: Proceedings of the proceedings of the dendrosymposium 2011, May 11th - 14th 2011, Orléans, France*, eds H. Gärtner, P. Rozenberg, P. Montès, O. Bertel, I. Heinrich, and G. Helle (Potsdam: GFZ-Potsdam), 28–40.
- van der Maaten-Theunissen, M. J., Boden, S., and van der Maaten, E. (2012). Wood density variations of Norway spruce (*Picea abies* (L.) Karst.) under contrasting climate conditions in southwestern Germany. *Ann. For. Res.* 56, 91–103.
- van der Maaten-Theunissen, M. J., and Bouriaud, O. (2012). Climate-growth relationships at different stem heights in silver fir and Norway spruce. *Can. J. For. Res.* 42, 958–969. doi: 10.1139/X2012-046
- van der Maaten-Theunissen, M. J., Kahle, H. P., and van der Maaten, E. (2013). Drought sensitivity of Norway spruce is higher than that of silver fir along an altitudinal gradient in southwestern Germany. *Ann. For. Sci.* 70, 185–193. doi: 10.1007/s13595-012-0241-0
- van Loo, M., and Dobrowolska, D. (2019). “History of introducing Douglas-fir to Europe,” in *Douglas-fir: An option for Europe*, eds H. Spiecker, M. Lindner, and J. K. Schuler (Joensuu: European Forest Institute), 21–29. doi: 10.1086/597603
- Vejpustková, M., and Čihák, T. (2019). Climate response of Douglas fir reveals recently increased sensitivity to drought stress in Central Europe. *Forests* 10:97. doi: 10.3390/f10020097
- Vitali, V., Büntgen, U., and Bauhus, J. (2017). Silver fir and Douglas fir are more tolerant to extreme droughts than Norway spruce in southwestern Germany. *Glob. Change Biol.* 23, 5108–5119. doi: 10.1111/gcb.13774
- Vitali, V., Büntgen, U., and Bauhus, J. (2018). Seasonality matters—The effects of past and projected seasonal climate change on the growth of native and exotic conifer species in Central Europe. *Dendrochronologia* 48, 1–9. doi: 10.1016/j.dendro.2018.01.001
- Vitasse, Y., Bottero, A., Rebetez, M., Conedera, M., Augustin, S., Brang, P., et al. (2019). What is the potential of silver fir to thrive under warmer and drier climate? *Eur. J. For. Res.* 138, 547–560. doi: 10.1007/s10342-019-01192-4
- Wassenberg, M., Chiu, H.-S., Guo, W., and Spiecker, H. (2015a). Analysis of wood density profiles of tree stems: Incorporating vertical variations to optimize wood sampling strategies for density and biomass estimations. *Trees* 29, 551–561. doi: 10.1007/s00468-014-1134-7
- Wassenberg, M., Schinker, M. G., and Spiecker, H. (2015b). Technical aspects of applying high frequency densitometry: Probe-sample contact, sample surface preparation and integration width of different dielectric probes. *Dendrochronologia* 34, 10–18. doi: 10.1016/j.dendro.2015.03.001
- Wassenberg, M., Montwé, D., Kahle, H. P., and Spiecker, H. (2014). Exploring high frequency densitometry calibration functions for different tree species. *Dendrochronologia* 32, 273–281. doi: 10.1016/j.dendro.2014.07.001